Available online at www.sciencedirect.com
SCIENCE DIRECT
Thermochimica Acta 441 (2006) 45–52
thermochimica acta
www.elsevier.com/locate/tca

Addition effect of erbium(III) trifluoromethanesulfonate in the homopolymerization kinetics of a DGEBA resin

S.J. García [a,*], X. Ramis [b], A. Serra [c], J. Suay [d]

[a] *Área de Ciencia de los Materiales, Departament d'Enginyeria de Sistemes Industrials i Disseny, Universitat Jaume I, Avda. Vicent Sos Baynat s/n, 12071 Castellón, Spain*
[b] *Laboratori de Termodinàmica, Escola Tècnica Superior Enginyeria Industrial Barcelona, Universitat Politècnica de Catalunya, Diagonal 647, 08028 Barcelona, Spain*
[c] *Departament de Q. Analítica i Q. Orgànica, Facultat de Química, Universitat Rovira i Virgili, C/Marcel·lí Domingo s/n, 43007 Tarragona, Spain*
[d] *Centro de Biomateriales, Universitat Politècnica de València, Camino de Vera s/n, E-46071 València, Spain*

Received 5 July 2005; received in revised form 16 November 2005; accepted 24 November 2005

Abstract

Solid bisphenol-A epoxy resin of medium molecular weight was cured using a Lewis acid initiator (erbium(III) trifluoromethanesulfonate) in three different proportions (0.5, 1 and 2 phr). A kinetic study was performed in a differential scanning calorimeter. The complete kinetic triplet was determined (activation energy, pre-exponential factor, and integral function of the degree of conversion) for each system. A kinetic analysis was performed with an integral isoconversional procedure (model-free), and the kinetic model was determined both with the Coats–Redfern method (the obtained isoconversional E value being accepted as the effective activation energy) and through the compensation effect. All the systems followed the same isothermal curing model simulated from non-isothermal ones. The "nucleation and growth" Avrami kinetic model $A_{3/2}$ has been proposed as the polymerization kinetic model. The addition of initiator accelerated the reaction having higher influence when low temperatures were applied.

Keywords: Epoxy resin; Initiator; Erbium triflate; Kinetics (polym.)

1. Introduction

The formulation of low curing temperatures epoxy powder coatings (using new initiator and crosslinkers) has become one of the main lines of research in industries and related research centres. One of the main objectives of the research is to obtain epoxy systems with low curing temperatures so that they can be applied on different substrates sensitive to temperature (mainly different types of organic ones like plastics), and of course to reduce energetic costs. Properties of the paints (mechanical, thermal, anticorrosive and so on) are specially influenced by the kind of epoxy network-structure (which depends on the crosslinker and initiator employed in its formulation).

Powder coatings are currently the fastest growing section of industrial paints, because of their favourable environmental attributes and performance advantages. They are well adapted for the main strategic goals of the paint industry, namely corrosion protection, improved durability, increased transfer efficiency, elimination of organic solvents, reduction of toxic waste, conservation of energy and reduction of costs. Since they are fully solid, and without volatile organic emissions, powder coatings are considered to be the best alternative for the reduction of the volatile organic contents (VOCs) of solvent-based paints, among the emerging coating technologies (powder coatings, high solid coatings and waterborne ones) [1,2].

Compared to liquid paints, the film formation process of powder coatings is different since it is occurring in the molten phase. Melting, flow, gel point and cure completion are the principal stages in film formation of powder coatings and determine both the aesthetic and protective properties of the paint. The duration of these stages is directly affected by the paint composition, e.g., type of binder and crosslinker, pigmentation (nature and particle size, packaging and distribution), initiator, and additives, curing and application conditions. These factors, in

* Corresponding author. Tel.: +34 964 728212.
E-mail address: espallar@sg.uji.es (S.J. García).

0040-6031/$ – see front matter © 2005 Elsevier B.V. All rights reserved.
doi:10.1016/j.tca.2005.11.043

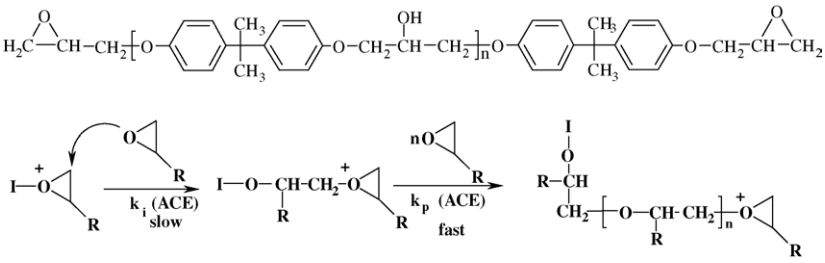

Scheme 1. Activated chain-end mechanism/ACE.

turn, determine important coating characteristics such as levelling, adhesion, gloss, chemical resistance and exterior durability [3–12].

Catalysts are important in polymerization processes because they decrease the activation energies and accelerate the reaction. They can be stimulated by heating or photoirradiation but, from the practical point of view, heating is the easier option; homogeneous heating of reaction mixtures can be achieved without difficulty [13]. In addition, elementary reactions are accelerated and the viscosity of the reaction mixture decreases. This shortens the reaction time, especially for systems in which the curing rate is diffusion-determined. Among the new thermal initiators, those having anions with low nucleophilicity, minimize or prevent the reaction of the growing chain with the anion, being more actives their cationic salts and more effective the polymerization [14].

The Lewis acid character and the great oxophilicity of lanthanide compounds is highly improved in the case of lanthanide triflates because of the electron-withdrawing capacity of the anionic group [15], which can coordinate to the epoxide oxygens weakening the C–O bond. Lewis acids, such as $AlCl_3$, BF_3 or $TiCl_4$ are moisture sensitive and easily decomposed or deactivated in the presence of humidity. On the contrary, lanthanide triflates are stable and work as Lewis acids in water. This fact represents an enormous advantage in their technological application as initiators.

As usual in Lewis acid initiators, erbium(III) trifluoromethanesulfonate leads to chain growth polymerization of epoxy compounds, which mainly proceed by the cationic chain end mechanism depicted in Scheme 1, where oxirane group of DGEBA resin is opened by coordination of oxirane oxygen to the cation and nucleophilic attack of another oxirane group.

Moreover, the presence of hydroxylic groups can lead to hydroxylic initiated polyetherification processes that can change both the kinetics of the reaction and the properties of the materials (Scheme 2), although this kind of reaction is less important in extension than the first one and, because of the low proportion of hydroxyls.

Nevertheless, the proportion of hydroxylic groups can influence the global propagation rate. In addition to these competitive growth chain mechanisms, inter and intra molecular transfer processes can occur and also termination reactions. All these processes lead to changes in the network structure and difficult the study of the kinetics of each one by separate. Thus, the kinetics of a cationic cure should be studied taking the process as a whole [16,17].

The usefulness of this type of initiator has been proved in other studies [14,18] with liquid epoxy resins, showing that the initiators highly accelerated the reactions of the system. Nevertheless, the behaviour of these initiators in powder coatings (using epoxy resins in the molten phase) has not yet been studied.

To predict the temperatures and times at which these polymerizations should be performed, one must know the kinetics. Preliminary kinetic studies have been performed using the method described by Kissinger [19]. This procedure, used by many authors because of its simplicity, assumes a reaction mechanism of order *n*. However, this assumption is not correct in many cases and leads to incorrect values of the pre-exponential factor *A*. In addition, kinetic methods that only use the maximum of the velocity curve to determine the kinetic parameters do not allow an assessment of whether these parameters vary during polymerization or not. Here we attempt to establish a method for this type of polymerization that allows the complete kinetic triplet (kinetic model, *E* and *A*) to be determined throughout the entire reaction. To analyze exothermic polymerizations, we have adapted a method from earlier studies addressing the kinetics of curing and degradation [20].

Many exothermic polymerizations present difficulties for the determination of the heat of reaction through isothermal experiments and deduction of the kinetics from these values. When reactions are performed at high temperatures, some of the heat may be lost during the stabilization of the apparatus, whereas at low temperatures, the heat is released slowly and can fall below the sensitivity of the calorimeter. Another problem arises when a physical phenomenon (e.g. fusion) over-

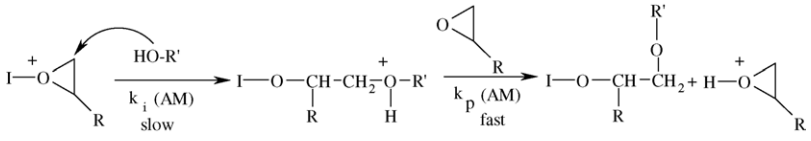

Scheme 2. Activated monomer mechanism/AM.

laps with the polymerization. One alternative in both cases is to simulate isothermal polymerization with non-isothermal data [21].

In this work a complete kinetic study of homopolymerization of DGEBA resin with erbium(III) trifluoromethanesulfonate as initiator has been developed. Isothermal polymerization was simulated with non-isothermal data. The reaction model was established from non-isothermal data with two different methods and proved with a posterior isothermal scan. The first method was the Coats–Redfern method [22], and the E value obtained isoconversionally was taken as the effective value. The second method used the compensation effect existing between E and A at the change in the degree of conversion (α) [20,23].

2. Experimental

2.1. Materials

Solid, bisphenol-A-based epoxy resin of medium molecular weight, 773 g/equiv. epoxy (from Huntsman), was homopolymerized with erbium(III) trifluoromethanesulfonate (from Aldrich) in three different amounts: 0.5, 1 and 2 phr (parts of initiator per hundred of resin, w/w).

Samples were premixed and hand-shacked until good mixing was afforded. After that, the material was extruded in a single screw extruder (Haake Rheomex 254), where operating conditions were 80 °C along the extruder and 60 rpm. Once extruded, the material was grinded in an ultra-centrifugal mill ZM 100 and sieved at 100 μm.

2.2. Testing methods and equipment

2.2.1. Differential scanning calorimeter (DSC)

A Perkin Elmer DSC 7 differential scanning calorimeter was employed for dynamic scans in order to study the non-isothermal curing process and to obtain the kinetic model parameters. The samples were analyzed in covered aluminium pans, using high purity indium sample for calibration. A flow of 20 $cm^3\ min^{-1}$ of argon was used as purge gas. The weigh of the samples was between 8 and 9 mg. Non-isothermal tests were performed at rates of 2.5, 5, 10 and 15 $K\ min^{-1}$ to not-cured-samples of epoxy systems using three different erbium triflate initiator amounts. The scans were performed at the range of temperature from 25 to 300 °C.

Isothermal scans at 120 °C were also performed in order to obtain the experimental isothermal conversion degree. Different samples were maintained at the isothermal temperature for different given times. After each isothermal scan, the sample was cooled until ambient temperature inside the calorimeter and followed by a dynamic scan in order to obtain the residual enthalpy. With these data and the total enthalpy obtained from a dynamic scan to a non-cured sample, the conversion degree was calculated.

STARe Mettler Toledo software was used in order to calculate conversion degrees and kinetics of the process. Kinetic analysis, using Coats–Redfern and IKR methods, was used to calculate the kinetic triplet.

2.2.2. Kinetic analysis

If we accept that the dependence of the rate constant on the temperature follows the Arrhenius equation, the kinetics of the reaction is usually described as follows:

$$r = \frac{\mathrm{d}\alpha}{\mathrm{d}t} = A \exp\left(-\frac{E}{RT}\right) f(\alpha) = k f(\alpha) \tag{1}$$

where t is the time, T the absolute temperature, R the gas constant, and $f(\alpha)$ is the differential conversion function.

Kinetic analysis has generally been performed with an isoconversional method. The basic assumption of such method is that the reaction rate at a constant conversion is solely a function of temperature [24].

2.2.2.1. Isothermal methods. By integrating the rate equation (1) under isothermal conditions, we obtain

$$\ln t = \ln\left[\frac{g(\alpha)}{A}\right] + \frac{E}{RT} \tag{2}$$

where $g(\alpha)$ is the integral conversion function. It is defined as follows:

$$g(\alpha) = \int_0^\alpha \frac{\mathrm{d}\alpha}{f(\alpha)} \tag{3}$$

According to Eq. (2), E and the constant $\ln[g(\alpha)/A]$ can be obtained from the slope and the intercept, respectively, of the linear relationship $\ln t = f(T^{-1})$ for a constant value of α.

2.2.2.2. Non-isothermal methods. When non-isothermal methods are applied, the integration of rate equation (1) and its reordering, gives place to the so-called temperature integral:

$$g(\alpha) = \int_0^\alpha \frac{\mathrm{d}\alpha}{f(\alpha)} = \frac{A}{\beta}\int_0^T \mathrm{e}^{-(E/RT)}\,\mathrm{d}T \tag{4}$$

where β is the heating rate.

By using the Coats–Redfern [22] approximation for the resolution of Eq. (4) and considering $2RT/E \ll 1$, we can rewrite this equation as follows:

$$\ln\frac{g(\alpha)}{T^2} = \ln\left[\frac{AR}{\beta E}\right] - \frac{E}{RT} \tag{5}$$

For a given kinetic model, the linear representation of $\ln[g(\alpha)/T^2]$ versus T^{-1} makes it possible to determine E (apparent E value) and A from the slope and the ordinate at the origin. In this work, the kinetic model that had the best linear correlation in the Coats–Redfern equation and that had an E value similar to that obtained isoconversionally (considered to be the effective E value) was selected.

By reordering Eq. (5), we can rewrite:

$$\ln\frac{\beta}{T^2} = \ln\left[\frac{AR}{g(\alpha)E}\right] - \frac{E}{RT} \tag{6}$$

The linear representation of $\ln[\beta/T^2]$ versus $1/T$ makes it possible to determine E and the kinetic parameter $\ln[AR/g(\alpha)E]$ for every value of α.

The constant $\ln[AR/g(\alpha)E]$ is directly related by the R/E to the constant $\ln[g(\alpha)/A]$ of the isothermal adjustment. Thus, taking the dynamic data $\ln[AR/g(\alpha)E]$ and E from Eq. (6), we can determine the isothermal parameters of Eq. (2) and simulate isothermal curing without knowing $g(\alpha)$ [25,26].

The STARe Mettler Software uses Eqs. (6) and (2) to determine the isonconversional activation energy and the isothermal times, respectively.

2.2.2.3. Compensation effect and isokinetic relationship (IKR). Complex processes are characterized by the dependences of E on A and α. This generally reflects the existence of a compensation effect through the following equation:

$$\ln A_\alpha = aE_\alpha + b = \frac{E_\alpha}{RT} + \ln\left[\frac{(d\alpha/dt)_\alpha}{f(\alpha)}\right] \quad (7)$$

where a and b are constants and subscript α represents the degree of conversion that produces a change in the Arrhenius parameters.

The slope $a = 1/RT_{iso}$ is related to the isokinetic temperature (T_{iso}), and the intercept $b = \ln k_{iso}$ is related to the isokinetic rate constant (k_{iso}). Eq. (7) represents an IKR and can be deduced by the reordering of Eq. (2). The appearance of the IKR shows that only one mechanism is present, whereas the existence of parameters that do not meet the IKR implies that there are multiple reaction mechanisms [27].

In this study, the kinetic model whose IKR had the best linear correlation between E and A and in which the associated T_{iso} value was near the experimental temperature range was selected [28]. The influence of more addition of erbium triflate in the kinetics of the system has been studied.

3. Results and discussion

In Fig. 1 it is shown the thermogram corresponding to the heating of three different samples with 0.5, 1 and 2 phr of erbium triflate, at a rate of 5 °C/min. The thermogram exhibits in the three cases a small endothermic peak at 60 °C (where the T_g should be detected) related with physical aging of the DGEBA and an exothermic one at higher temperatures (near 120 °C) related to the curing reaction of the epoxy resin. It can be seen that for the three different samples, similar curve thermograms were obtained. As the content in erbium triflate increases, the thermogram shifts to minor temperatures. The reaction heat is almost constant at 105 kJ/mg for all the samples.

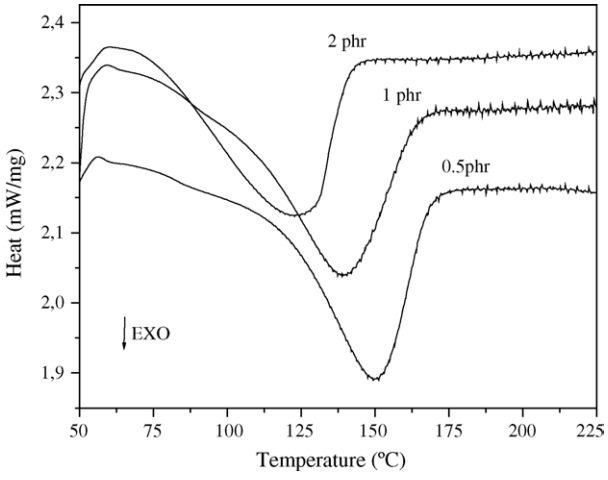

Fig. 1. Non-isothermal DSC thermograms at 5 °C/min of heating rate for three different epoxy systems containing 0.5, 1 and 2 phr of erbium triflate.

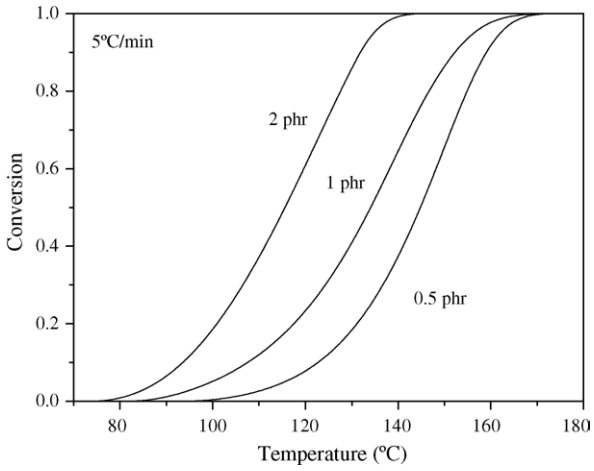

Fig. 2. Conversion degree (α) vs. temperature plots for a heating rate of 5 °C/min for three different epoxy systems containing 0.5, 1 and 2 phr of erbium triflate as initiator.

The results of the calorimetric scannings were employed to obtain the conversion degree with temperature, by means of the STARe software. Fig. 2 shows α versus T plots for a constant rate of 5 °C/min for the three samples used. It can be seen that the higher the content in erbium triflate, the lower the temperature for a given conversion degree is.

In Fig. 3, it is plotted the influence of the heating rate for a sample with 1 phr of erbium triflate obtained with STARe software. It can be seen that as the rate of heating increases, the thermogram shifts to higher temperatures.

The non-isothermal isoconversional kinetic parameters were calculated from the α–T curves by the application of Eq. (6) to different conversions, and from these, the isothermal parameter

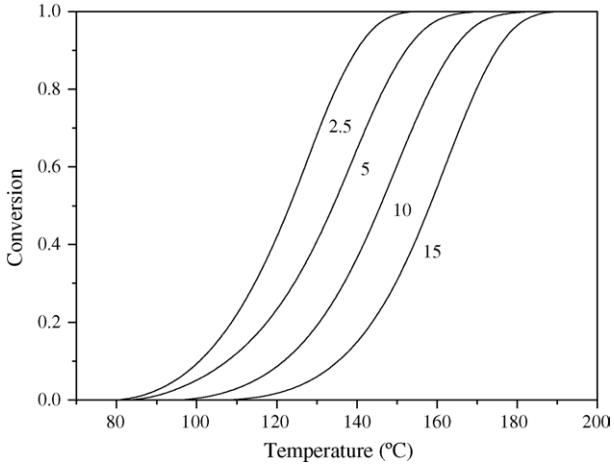

Fig. 3. Conversion degree (α) for an epoxy system with 1 phr of erbium triflate as initiator at different heating rates (2.5, 5, 10 and 15 °C/min).

Table 1
Kinetic parameters of non-isothermal homopolymerization obtained by Eq. (6), for a sample with 1 phr of erbium triflate

α	E (kJ/mol)[a]	$\ln[AR/g(\alpha)E]$ (K^{-1} min^{-1})[a]	$\ln[g(\alpha)/A]$ (min)[b]	$\ln A$ (min^{-1})[c]	r
0.1	71.3	12.34	−21.39	19.89	0.968
0.2	74.6	12.80	−21.91	20.91	0.982
0.3	76.9	13.16	−22.29	21.60	0.987
0.4	79.0	13.48	−22.64	22.19	0.989
0.5	80.6	13.71	−22.89	22.64	0.990
0.6	81.8	13.82	−23.02	22.96	0.992
0.7	82.7	13.83	−23.04	23.16	0.993
0.8	83.7	13.89	−23.11	23.43	0.994
0.9	85.3	14.03	−23.27	23.82	0.996

[a] $\ln[AR/g(\alpha)E]$ and E were calculated on the basis of non-isothermal DSC experiments as the intercept and slope of the isoconversional relationship $\ln[\beta/T^2] = \ln[AR/g(\alpha)E] - E/RT$.
[b] $\ln[g(\alpha)/A]$ was calculated on the basis of $\ln[AR/g(\alpha)E]$ and E.
[c] $\ln A$ was calculated with kinetic model $A_{3/2}$ and $\ln[g(\alpha)/A]$.

Table 2
Algebraic expressions for $f(\alpha)$ and $g(\alpha)$ for the kinetic models used

Models	$f(\alpha)$	$g(\alpha)$
$A_{3/2}$	$(3/2)(1-\alpha)[-\ln(1-\alpha)]^{1/3}$	$[-\ln(1-\alpha)]^{2/3}$
A_2	$2(1-\alpha)[-\ln(1-\alpha)]^{1/2}$	$[-\ln(1-\alpha)]^{1/2}$
A_3	$3(1-\alpha)[-\ln(1-\alpha)]^{2/3}$	$[-\ln(1-\alpha)]^{1/3}$
A_4	$4(1-\alpha)[-\ln(1-\alpha)]^{3/4}$	$[-\ln(1-\alpha)]^{1/4}$
R_2	$2(1-\alpha)^{1/2}$	$1-(1-\alpha)^{1/2}$
R_3	$3(1-\alpha)^{2/3}$	$1-(1-\alpha)^{1/3}$
D_1	$(2\alpha)^{-1}$	α^2
D_2	$[-\ln(1-\alpha)]^{-1}$	$(1-\alpha)\ln(1-\alpha)+\alpha$
D_3	$(3/2)(1-\alpha)^{2/3}[1-(1-\alpha)^{1/3}]^{-1}$	$[1-(1-\alpha)^{1/3}]^2$
D_4	$(3/2)(1-\alpha)^{1/3}[1-(1-\alpha)^{1/3}]^{-1}$	$(1-2/3\alpha)(1-\alpha)^{2/3}$
F_1	$(1-\alpha)$	$-\ln(1-\alpha)$
Power	$2\alpha^{1/2}$	$\alpha^{1/2}$
$n+m=2$; $n=1.9$	$\alpha^{0.1}(1-\alpha)^{1.9}$	$[(1-\alpha)\alpha^{-1}]^{-0.9}(0.9)^{-1}$
$n+m=2$; $n=1.5$	$\alpha^{0.5}(1-\alpha)^{1.5}$	$[(1-\alpha)\alpha^{-1}]^{-0.5}(0.5)^{-1}$
$n=2$	$(1-\alpha)^2$	$-1+(1-\alpha)^{-1}$
$n=3$	$(1-\alpha)^3$	$2^{-1}[-1+(1-\alpha)^{-2}]$

$\ln[g(\alpha)/A]$, with which the studied curing process would subsequently be simulated. Table 1 shows the results obtained for the sample prepared at 1 phr of erbium triflate using the 5 °C/min calorimetric signal. The process was repeated with the other proportions of triflate.

Fig. 4 shows the experimental relationship between $\ln[\beta/T^2]$ and the inverse of temperature, with the adjustment made with Eq. (6). Table 1 shows that E is weakly modified during homopolymerization, rising with the advance of the reaction, probably due to the increased viscosity of the reaction medium as the molecular weight increases. The parameters $\ln[AR/g(\alpha)E]$ and the associated A values exhibit the same trend as E. The same results were obtained for the other two proportions.

To establish the kinetic model for the system with an initiator amount of 1 phr, the isoconversional kinetic parameters (Table 1) and the Eq. (7) were used (the same process was done for the other two systems). From the parameters $\ln[AR/g(\alpha)E]$ and E shown in Table 1 and the $g(\alpha)$ functions, A values were calculated for all the different kinetic models used (see Table 2).

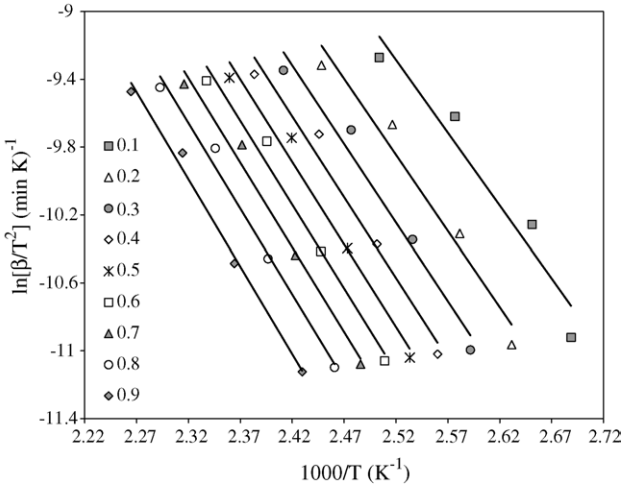

Fig. 4. Correlations between $\ln[\beta/T^2]$ and the inverse of the temperature (1000/T) for different values of α of an epoxy sample with 1 phr of erbium triflate.

Subsequently, by plotting E against $\ln A$, we determined the IKRs for all the models (Eq. (7)). Table 3 shows the obtained results, as well as the T_{iso} values determined from slope a of the IKRs. Although some models exhibit IKRs, the model considered that the best one describing the homopolymerization is the nucleation growth type of Johnson, Male, Avrami, Kolmogorov and Yerofeev, $JMAKY_{3/2}$ (from here on, named as Avrami $A_{3/2}$ in order to simplify [29]) because this model shows the best regression and has a T_{iso} value close to the experimental temperatures. In agreement with Vyazovkin and Linert [28], a T_{iso} value close to the range of experimental temperatures indicates that the kinetic model accurately describes the reactive process. The same conclusion was obtained for the systems with 0.5 and 2 phr of erbium triflate.

To confirm the methodology used, we determined E and $\ln A$ for each of the tested models with the Coats–Redfern method (Eq. (5)). The results obtained for the rate of 5 °C/min for the sample with 1 phr of erbium triflate when Eq. (5) was applied to conversions between 0.2 and 0.8 are shown in Table 3 (other tested rates showed similar results). The same process was applied to the other two samples. Some of the models exhibit very good regressions, and so from these data alone, it is not possible to establish the reaction mechanism. To determine the kinetic model, it was also used the mean value of E obtained isoconversionally (79.9 kJ/mol; Table 1). This value of E is considered the effective value because it was obtained without the necessity of determining the model. In addition to exhibiting a good regression, the correct kinetic model must also possess a value of E similar to the effective value. According to these criteria, model $A_{3/2}$ with $r = 0.9999$ and $E = 54.88$ kJ/mol, is considered the correct one even if the E values is lower than that found with the isoconversional (Table 5). Other models like R3 and F1 could also describe the process, but taking into account that the three systems using erbium triflate must show the same model, it was chosen that one representing all the systems and having good regression in all cases. In Table 4 it can be seen the Coats–Redfern results for the other two samples and how the kinetic model chosen is valid for all the systems.

Table 3
Arrhenius parameters determined by the Coats–Redfern method and isokinetic parameters for a sample with 1phr of erbium triflate

Models	Coats–Redfern (1 phr)			IKR (1 phr)			
	E (kJ/mol)	$\ln A$ (min^{-1})	r	a (mol/kJ)	b (min^{-1})	T_{iso} (°C)	r
$A_{3/2}$	54.88	14.362	0.9999	0.2807	−0.039	155.55	0.9990
A_2	39.47	9.541	0.9999	0.2447	2.902	218.49	0.9983
A_3	24.07	4.555	0.9999	0.2088	5.843	303.09	0.9970
A_4	16.37	1.924	0.9998	0.1908	7.313	357.34	0.9959
R_2	71.34	18.484	0.9994	0.3304	−5.402	91.00	0.9982
R_3	75.89	19.549	0.9998	0.3204	−4.177	102.45	0.9971
D_1	124.69	34.596	0.9968	0.4507	−14.999	−6.12	0.9937
D_2	146.53	41.551	0.9989	0.4830	−18.034	−23.98	0.9966
D_3	158.52	43.113	0.9998	0.5240	−22.529	−43.45	0.9990
D_4	146.14	39.203	0.9993	0.4965	−20.521	−30.73	0.9976
F_1	85.68	23.790	0.9999	0.3525	−5.921	68.17	0.9996
Power	26.12	4.999	0.9953	0.2154	5.044	285.53	0.9921
$n+m=2$; $n=1.9$	107.68	31.053	0.9955	0.4046	−9.467	24.28	0.9968
$n+m=2$; $n=1.5$	56.83	15.946	0.9951	0.2856	0.586	148.11	0.9994
$n=2$	120.40	34.824	0.9956	0.4343	−11.938	3.92	0.9961
$n=3$	162.46	48.051	0.9885	0.5356	−19.413	−48.41	0.9832

All the samples have shown that the two methodologies produce the same result, and in both cases, it is necessary to know the effective E (isoconversional) value to determine the complete kinetic triplet (E_a, A and $f(\alpha)$).

If we compare the activation energies (Table 5), a simple analysis would conclude that the fastest system is that with the major E_a, but this is not always true because it exist a compensation effect between E and $\ln A$. Then, to know which system is the most efficient it should be compared the conversion rate r. Eq. (8) shows the Arrhenius relation between k (rate constant), A and E:

$$k = A\exp\left(-\frac{E}{RT}\right) \rightarrow \ln k = \ln A - \frac{E}{RT} \tag{8}$$

From Eq. (1),

$$\ln r = \ln A - \frac{E}{RT} + \ln f(\alpha) \tag{9}$$

Table 5
Variation of the activation energy with the conversion of samples with 0.5, 1 and 2 phr of erbium triflate

Conversion	E_a (kJ/mol)		
	0.5 phr	1 phr	2 phr
0.1	53.8	71.3	61.4
0.2	59.6	74.6	61.5
0.3	62.7	76.9	62.2
0.4	64.6	79.0	63.5
0.5	66.0	80.6	65.4
0.6	67.1	81.8	67.7
0.7	67.9	82.7	70.4
0.8	68.6	83.7	73.3
0.9	69.3	85.3	75.1

Table 4
Arrhenius parameters determined by the Coats–Redfern method for samples with 0.5 and 2 phr of erbium triflate

Models	Coats–Redfern (0.5 phr)			Coats–Redfern (2 phr)		
	E (kJ/mol)	$\ln A$ (min^{-1})	r	E (kJ/mol)	$\ln A$ (min^{-1})	r
$A_{3/2}$	72.37	19.207	0.9998	53.69	14.830	0.9998
A_2	52.55	13.240	0.9998	38.66	9.913	0.9997
A_3	32.72	7.120	0.9998	23.63	4.827	0.9997
A_4	22.81	3.936	0.9998	16.49	2.171	0.9996
R_2	162.27	44.684	0.9995	69.56	18.994	0.9981
R_3	188.60	52.810	0.9994	74.07	20.108	0.9990
D_1	205.76	55.724	0.9971	121.14	35.297	0.9943
D_2	189.83	50.889	0.9990	142.49	42.314	0.9974
D_3	93.57	24.563	0.9999	154.58	44.166	0.9991
D_4	99.43	25.968	0.9994	142.32	40.122	0.9979
F_1	112.01	30.938	0.9998	83.76	24.457	0.9998
Power	35.38	7.718	0.9960	25.46	5.223	0.9918
$n+m=2$; $n=1.9$	140.30	39.843	0.9952	105.73	32.021	0.9971
$n+m=2$; $n=1.5$	74.87	20.934	0.9948	55.88	16.516	0.9968
$n=2$	156.66	44.565	0.9952	118.19	35.891	0.9971
$n=3$	210.77	60.939	0.9878	159.98	49.618	0.9910

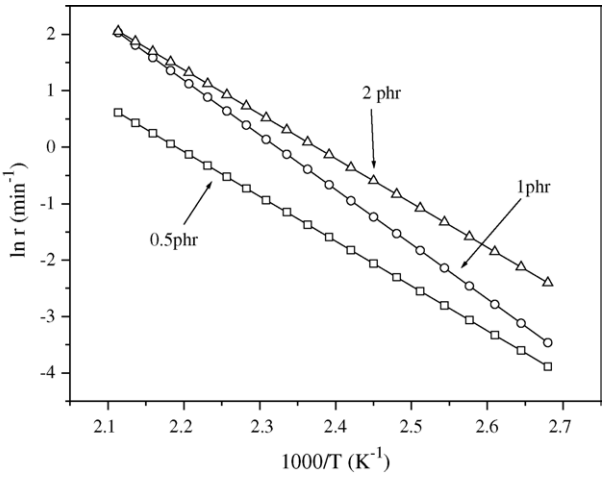

Fig. 5. Conversion rate ($\ln r$) vs. the inverse of the temperature (1000/T) for samples with 0.5, 1 and 2 phr of erbium triflate.

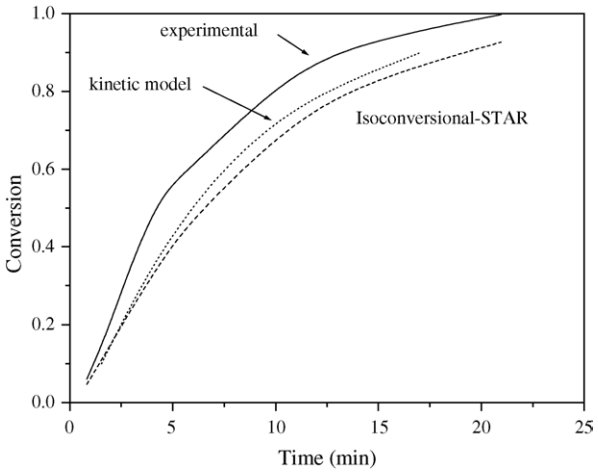

Fig. 6. Conversion vs. time graphics of data obtained experimentally (isothermally at 120 °C), isoconversionally with the STAR software and from the chosen kinetic model for a sample with 1 phr of erbium triflate.

Introducing in this equation values of E, A and α with the chosen kinetic model $A_{3/2}$ and for a given conversion degree ($\alpha = 0.5$) we can obtain a graphic like Fig. 5 ($\ln r = f(1/T)$).

In this figure it can be observed that, when introducing more initiator the faster the system is. As temperature raises, the conversion rate of the systems with 1 and 2 phr of erbium initiator get closer, meaning that the system is almost not accelerated when introducing initiator over 1 phr when high temperatures are used (e.g. 200 °C). But when low temperatures are used, significant acceleration of the system is shown (e.g. 100 °C) when more initiator is added. These results corroborate that in order to know which system is the fastest; it is appropriate to consider not only E_a but also the parameter $\ln A$ if the kinetic models are the same.

In order to know whether the kinetic model chosen and isoconversional data obtained by the STAR software fitted the experimental data or not a comparison between conversion-time graphics for a given temperature was made. Because isothermal reactions of these systems were very fast, the DSC equipment was not able to detect the initial calorimetric signal because stabilization time is needed and the initial part of the cure was lost.

The experimental conversion degree (α) data were obtained doing a first isothermal test during a given time in a DSC, afterwards a scan from 25 to 300 °C at 5 °C/min was performed for each isothermal test. With Eq. (10) and the residual enthalpies obtained, the different conversion values where calculated:

$$\alpha_{exp} = \frac{\Delta H_{total} - \Delta H_{residual}}{\Delta H_{total}} \quad (10)$$

where $\Delta H_{tot} = 73.3$ kJ/equiv. epoxy obtained from non-isothermal data.

Fig. 6 represents the three curves obtained: kinetic model data, isoconversional data obtained by the STAR software and finally experimental data, for a sample with 1 phr of erbium triflate.

It can be observed that the three curves show the same trend, although experimental data present shorter times for the same conversion. These shorter experimental times at a given temperature compared to the modelled data can be due either to the fact that the epoxy curing process could not exactly be the same under isothermal or non-isothermal tests, or to some experimental problems in the calorimeter. Firstly, the DSC needs a short time to bring the sample to the isothermal curing temperature, meaning that the curing reaction begins before reaching the isothermal temperature. Secondly, when the isothermal test finishes the cooling of the sample in the calorimeter is not immediate, so again some time is needed to decrease the temperature and the reaction process continues until ambient temperature is reached, probably non-isothermal data give more accurate results than these isothermal experiments.

Nevertheless, as the curves are very similar it can be pointed out that the kinetic model chosen fits quite well the isoconversional data obtained with STAR software and experimental data.

4. Conclusions

To compare kinetic results, it is necessary to know the complete kinetic triplet (E, A, $g(\alpha)$) because of the existence of a compensation effect between E and $\ln A$. The use of E as a unique comparative parameter can introduce errors.

Two methods that allow the determination of the complete kinetic triplet have been shown, as well as the simulation of the polymerization. Both methods require the effective E value to be known, which can be determined with an isoconversional procedure (model-free).

An epoxy system composed by a DGEBA resin and a Lewis acid initiator (erbium(III) trifluoromethanesulfonate with applications in the formulation of low curing powder coatings) was studied. Three different amounts of initiator were prepared: 0.5, 1 and 2 phr. A kinetic study by means of non-isothermal tests in a DSC was carried out and a posterior isokinetic study was developed. All systems showed that the reaction mechanism followed an $A_{3/2}$ "nucleation and growth" model, showing no dependence on the initiator amount.

Reaction rates for all the systems were obtained. Results showed that the more the initiator is added, the faster the reaction

rate is, but when high temperatures were used, the differences in the conversion degree decreased.

A simulation of the isothermal curing to a reasonably accurate degree has been obtained. In this way it has been possible to obtain the isothermal curing degree versus temperature and time without any isothermal tests (that in fast catalyzed curing systems are experimentally difficult to perform) but only with four DSC dynamic scans at different rates.

Acknowledgements

Authors would like to thank Ms Eva Romero for her help in the development of this project. The authors from the Universitat Jaume I and Universitat Politècnica de València are grateful for the economic support in this work of CICYT MAT 2000-0123-P4-03. The author from the Universitat Rovira i Virgili would like to thank the CICYT-FEDER MAT2002-00291 and CIRIT SGR 00318 projects. Author from the Universitat Politècnica de Catalunya would like to thank CICYT and FEDER MAT2004-04165-C02-02 for their financial support.

References

[1] E. Bodner, Eur. Coat. Technol. 44 (1987).
[2] S.S. Lee, et al., Prog. Org. Coat. 36 (1999) 79–88.
[3] E.G. Belder, H.J.J. Rutten, D.Y. Perera, Cure characterization of powder coatings, Prog. Org. Coat. 42 (2001) 142–149.
[4] J. Hess, Powder powder everywhere, in: Coatings World, vol. 36, 1999.
[5] T.A. Misec (Ed.), Powder Coatings Chemistry and Technology, Wiley, New York, 1991.
[6] R. van der Linde, B.J.R. Scholtens, E.G. Belder, Proceedings of the 11th International Conference on Organic Coatings in Science and Technology, Athens, Greece, 1985, p. 147.
[7] F.M. Witte, C.D. Goemans, R. van der Linde, D.A. Stanssens, Prog. Org. Coat. 32 (1997) 241.
[8] M. Osterhold, F. Niggemann, Prog. Org. Coat. 33 (1998) 55.
[9] M. Johansson, H. Falken, A. Irestedt, A. Hult, J. Coat. Technol. 70 (884) (1998) 57.
[10] S.S. Lee, H.Z.Y. Han, J.G. Hilborn, J.-A.E. Manson, Prog. Org. Coat. 36 (1999) 79.
[11] R. van der Linde, E.G. Belder, D.Y. Perera, in: Proceedings of the 25th International Conference on Organic Coatings in Science and Technology, vol. 15, Athens, Greece, Prog. Org. Coat. 40 (2000) 215.
[12] D. Maetens, L. Moens, L. Boogaerts, K. Buysens, Eur. Coat. J. 25 (1999).
[13] T. Endo, F. Sanda, Macromol. Symp. 107 (1996) 237.
[14] C. Mas, A. Serra, A. Mantecón, J.M. Salla, X. Ramis, Macromol. Chem. Phys. 202 (2001) 2554–2564.
[15] S. Kobayashi, Synlett (1996) 689.
[16] L. Matejka, P. Chabanne, L. Tighzert, J.P. Pascault, J. Polym. Sci., Part A: Polym. Chem. 32 (1994) 1447–1458.
[17] P. Chabanne, L. Tighzert, J.P. Pascault, J. Appl. Polym. Sci. 53 (1994) 769–785.
[18] P. Castell, M. Galià, A. Serra, J.M. Salla, X. Ramis, Polymer 41 (2000) 8465.
[19] H.E. Kissinger, Anal. Chem. 29 (1957) 1702.
[20] X. Ramis, J.M. Salla, C. Mas, A. Mantecón, A. Serra, J. Appl. Polym. Sci. 92 (2004) 381.
[21] X. Ramis, J.M. Salla, J. Puiggalí, J. Polym. Sci., Part A: Polym. Chem. 43 (2005) 1166–1176.
[22] A.W. Coats, J. Redfern, Nature 207 (1964) 290.
[23] S. Vyazovkin, W. Linert, Int. Rev. Phys. Chem. 14 (1995) 355.
[24] S. Vyazovkin, C.A. Wight, Annu. Rev. Phys. Chem. 48 (1997) 125.
[25] X. Ramis, A. Cadenato, J.M. Salla, J.M. Morancho, A. Vallés, L. Contat, A. Ribes, Polym. Degrad. Stabil. 86 (2004) 483.
[26] X. Ramis, J.M. Salla, A. Cadenato, J.M. Morancho, J. Therm. Anal. Calorim. 72 (2003) 707.
[27] S. Vyazovkin, W. Linert, J. Solid State Chem. 114 (1995) 392.
[28] S. Vyazovkin, W. Linert, Chem. Phys. 193 (1995) 109.
[29] J. Sestak, Thermal Analysis in Thermophysical Properties of Solids, Elsevier, Amsterdam, 1984.